Proceedings of ICNMM2007
Fifth International Conference on Nanochannels, Microchannels and Minichannels
June 18-20, 2007, Puebla, Mexico

DRAFT **ICNMM2007-30060**

LATTICE BOLTZMANN METHOD FOR STEADY GAS FLOWS IN MICROCHANNELS WITH IMPOSED SLIP WALL BOUNDARY CONDITION

Seckin Gokaltun*
Applied Research Center
Florida International University
10555 W. Flagler St., EC 2100
Miami, FL 33174
Email: gokaltun@fiu.edu

George S. Dulikravich
Department of Mechanical and Materials Engineering
Multidisciplinary Analysis, Inverse Design,
Robust Optimization and Control (MAIDROC) Lab.
Florida International University
10555 W. Flagler St., EC 3474
Miami, FL 33174
Email: dulikrav@fiu.edu

ABSTRACT

In this paper, we use a lattice Boltzmann model (LBM) for simulation of rarefied gas flows in microchannels at high and moderate Knudsen numbers. The lattice Boltzmann method uses D2Q9 lattice structure and BGK collision operator with single relaxation time. The solid wall boundary conditions used in this paper are based on the idea of bounceback of the non-equilibrium part of particle distribution in the normal direction to the boundary. The same idea is implemented at inlet and exit boundaries as well as at the wall surfaces. The distribution functions at the solid nodes are modified according to imposed density and slip velocity values at the wall boundaries. Simulation results are presented for microscale Couette and Poiseuille flows. The results are validated against analytical and/or experimental data for the slip velocity, nonlinear pressure drop and mass flow rate at various flow conditions. It was observed that the current application of LBM can accurately recover the physics of microscale flow phenomena in microchannels. The type of boundary treatment used in this study enables the implementation of coupled simulations where the flow properties at the regions near the wall can be obtained by other numerical methods such as the Direct Simulation Monte Carlo method.

*Address all correspondence to this author.

INTRODUCTION

With the advances in micromachining technology it has been possible to manufacture micron sized devices with high precision. When the characteristic length scale in a microsystem becomes comparable to the mean free path (λ) the flow becomes rarefied. The rarefaction of the flow is described using the non-dimensional parameter called the Knudsen number, which is given as $Kn = \frac{\lambda}{H}$ where $\lambda = \frac{\kappa T}{P\sigma^2\pi\sqrt{2}}$ is the mean free path and H is the characteristic length. According to Bird [1], rarefied gas flows are classified into slip flow for $0.01 < Kn < 0.1$, and transition flow for $0.1 < Kn < 10$. For $Kn < 0.01$ the fluid can be considered as a continuum, whereas for $Kn > 10$ it is considered to be in free molecular regime.

Recently, the lattice Boltzmann method (LBM) became a popular molecular-based modeling tool that can be used to simulate rarefied gas flow for the whole flow regime [2]. Nie *et al.* [3] applied the LBM method for microchannel flows and showed that LBM can capture behaviors such as velocity slip, nonlinear pressure distribution along the channel and dependence of mass flow rate on Knudsen number. Using a specular bounce back boundary condition, Lim *et al.* [4] showed that LBM results for the slip microchannel flow were in good agreement with experimental data for pressure distributions. It was also observed by Zhang *et al.* [5] that LBM can predict the correct trend of mass flow rate as the Knudsen number increases along the microchannel.

The purpose of this study is to examine the steady gas flow in microchannels using a lattice Boltzmann method with imposed wall boundary conditions. First the LBM method used in this work is summarized and modifications for rarefied flows is discussed. Next the numerical test cases is described and the boundary conditions are specified. The pressure distribution, velocity profiles and mass flow rates are presented in the results section.

LATTICE-BOLTZMANN METHOD (LBM)

The LBM model used in this study follows the evolution of density distribution function f_a by calculating the lattice Boltzmann equation with streaming and single relaxation time BGK (Bhatnagar-Gross-Krook) collision operator [6]

$$f_a(\mathbf{x}+\mathbf{e_a}\Delta t, t+\Delta t) = f_a(\mathbf{x},t) - \frac{\Delta t}{\tau}\left(f_a(\mathbf{x},t) - f_a^{eq}(\mathbf{x},t)\right). \quad (1)$$

In Eq. (1), $\mathbf{x}$ denotes the position vector and a stands for one of the 9 possible directions on the D2Q9 lattice structure shown in Fig. 1. The components of the equilibrium distribution function f_a^{eq} are given by

$$f_a^{eq}(\mathbf{x}) = w_a \rho(\mathbf{x}) \left[1 + 3\frac{\mathbf{e}_a \cdot \mathbf{u}}{c^2} + \frac{9}{2}\frac{(\mathbf{e}_a \cdot \mathbf{u})^2}{c^4} - \frac{3}{2}\frac{\mathbf{u^2}}{c^2}\right] \quad (2)$$

where $w_a = 1/9$ for $a = 1-4$, $w_a = 1/36$ for $a = 5-8$ and $w_9 = 4/9$. In Fig. 1, particles move along 9 specific directions with speed

$$\mathbf{e_a} = \begin{cases} (\cos[(a-1)\frac{\pi}{2}], \sin[(a-1)\frac{\pi}{2}])c & a = 1-4 \\ (\cos[(a-5)\frac{\pi}{2}+\frac{\pi}{4}], \sin[(a-5)\frac{\pi}{2}+\frac{\pi}{4}])c & a = 5-8 \\ (0,0) & a = 9 \end{cases} \quad (3)$$

The ninth velocity is zero which stands for the particles at rest. The length scale (1 lu) is fixed by the distance between nodes.

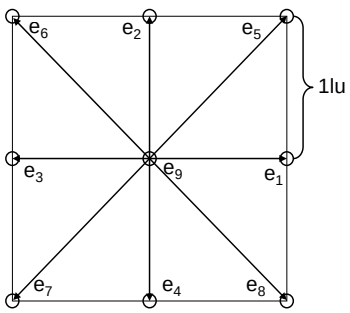

Figure 1. THE D2Q9 LATTICE STRUCTURE.

The procedure of LBM method can be summarized in two steps. First step is the collision step where the direction-specific density distributions are relaxed toward quasi-equilibrium distributions. At the second step, streaming, the distribution functions are moved to neighboring nodes. In the isothermal LBM model used here, the macroscopic density and velocity of particles at $\mathbf{x}$ is found by Eq. (4) given as

$$\rho = \sum_a f_a, \quad \rho\mathbf{u} = \sum_a \mathbf{e_a} f_a. \quad (4)$$

The pressure is related to density by $p = \rho c^2/3$ where the particle streaming speed is taken as $c = 1$. The LBM simulation is initialized by assigning a value for f_a at all lattice nodes in the domain, then the effects of boundary conditions and forces (if any) are incorporated. Finally, the equilibrium distributions are recomputed by Eq. (2), and the macroscopic flow properties are calculated at the next time step using Eq. (4).

For nearly incompressible flows the D2Q9 model is used with single relaxation time ($\tau = 1$). However, for rarefied gas flows in channels, compressibility effects must be taken into account and the relaxation time has to be modified [3]. In this work, the dimensionless relaxation parameter τ in Eq. 1 has been replaced with τ' according to Nie et al: [3]

$$\tau' = \frac{1}{2} + \frac{1}{\rho}(\tau - \frac{1}{2}). \quad (5)$$

The Knudsen number is calculated by [3]

$$Kn = \frac{a(\tau - 0.5)}{\rho H}, \quad (6)$$

Previous studies [7] has shown that it is acceptable to specify the coefficient as $a = 0.835$ in Eq. 6.

Boundary conditions

Most of the microchannel flows are induced by a pressure gradient where constant pressure values are speficied at the inlet and the exit. In our LBM model, we have used the idea of bounce-back of non-equilibrium part of the particle distribution function proposed by Zou and He [8] to achieve a pressure gradient in our microchannel simulations. To specify the pressure at the inlet, we assume that the velocity component normal to the inlet boundary is zero ($v_{in} = 0$) and the density is known (ρ_{in}). After streaming, at the inlet boundary f_2, f_3, f_4, f_6, f_7 are known as shown with solid arrows in Fig. 2. Using Eq. 4, the axial component of velocity at the inlet u_{in} and unknown density functions

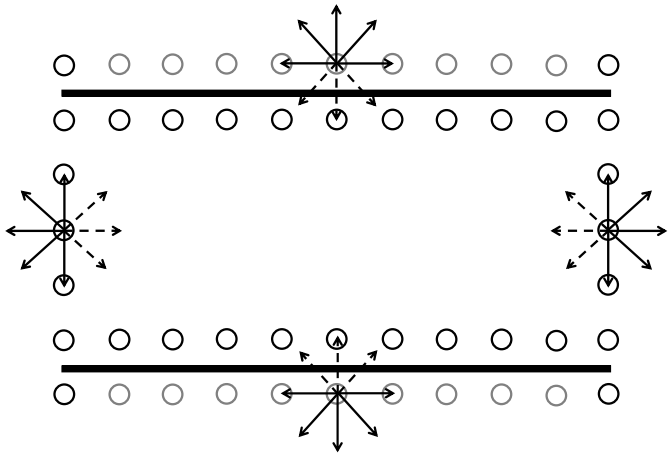

Figure 2. IMPLEMENTATION OF BOUNDARY CONDITIONS AT OUTER NODES.

f_1, f_5, f_8 are calculated as follows:

$$f_1 + f_5 + f_8 = \rho_{in} - (f_9 + f_2 + f_3 + f_4 + f_6 + f_7), \quad (7)$$
$$f_1 + f_5 + f_8 = \rho_{in} u_{in} + (f_3 + f_6 + f_7), \quad (8)$$
$$f_5 - f_8 = -f_2 f_4 - f_6 + f_7, \quad (9)$$

which in turn gives

$$u_{in} = 1 - \frac{[f_9 + f_2 + f_4 + 2(f_3 + f_6 + f_7)]}{\rho_{in}}, \quad (10)$$

Using the bounce-back rule for the non-equilibrium part normal to the inlet, $f_1 - f_1^{eq} = f_3 - f_3^{eq}$, we get

$$f_1 = f_3 + \frac{2}{3}\rho_{in} u_{in}. \quad (11)$$

With f_1 known, Eq. (8,9) give the rest of unknown functions

$$f_5 = f_7 - \frac{1}{2}(f_2 - f_4) + \frac{1}{6}\rho_{in} u_{in}, \quad (12)$$
$$f_8 = f_6 + \frac{1}{2}(f_2 - f_4) + \frac{1}{6}\rho_{in} u_{in}. \quad (13)$$

Assuming $v_{out} = 0$ and ρ_{out} is known, the same approach is used at the exit boundary to obtain the unknown values as

$$u_{out} = -1 + \frac{[f_9 + f_2 + f_4 + 2(f_1 + f_5 + f_8)]}{\rho_{out}}, \quad (14)$$
$$f_3 = f_1 - \frac{2}{3}\rho_{out} u_{out}, \quad (15)$$
$$f_6 = f_8 - \frac{1}{2}(f_2 - f_4) - \frac{1}{6}\rho_{out} u_{out}, \quad (16)$$
$$f_7 = f_5 + \frac{1}{2}(f_2 - f_4) - \frac{1}{6}\rho_{out} u_{out}. \quad (17)$$

For boundary conditions on the wall surfaces the similar approach is used assuming that the fluid properties are continuous from the interior flow field to the solid boundary. The normal velocity component is taken as zero at top and bottom boundaries, $v_t = v_b = 0$. If the density and axial velocity at the outer nodes can be estimated the unknown functions can be found. In our LBM analysis, we place the wall surface between the outer node and the neighbor node as shown in Fig. 2, so the outer top and bottom nodes are classified as solid nodes. In the current wall boundary condition the imposed values of density and velocity will be referred to effective density, ρ_{eff}, and effective velocity, u_{eff}, from this point on. For the top wall boundary this gives

$$f_4 = f_2 - \frac{2}{3}\rho_{eff} v_t, \quad (18)$$
$$f_8 = f_6 - \frac{1}{2}(f_1 - f_3) - \frac{1}{6}\rho_{eff} v_t + \frac{1}{2}\rho_{eff} u_{eff}, \quad (19)$$
$$f_7 = f_5 + \frac{1}{2}(f_1 - f_3) - \frac{1}{6}\rho_{eff} v_t - \frac{1}{2}\rho_{eff} u_{eff} \quad (20)$$

whereas the treatment for the bottom wall boundary is straightforward.

Results and Discussion

In this section, isothermal rarefied microchannel flows in two dimensions are investigated. The first case in our validation models is a planar Couette flow between two parallel plates. A channel with aspect ratio ($L/H = 20$) is used with upper plate moving initially at $u_t = 0.001$ while the lower one moves in the opposite direction at the same speed. The effective velocity at the solid node at the outer boundary is calculated as $u_{eff} = 2u_t - u(Ny-1)$. A periodic boundary condition is applied at the inlet and outlet. The velocity profiles across the distance between two plates for micro-Couette flow at $Kn = 0.05135$, $Kn = 0.5135$ and $Kn = 5.135$ are plotted in Fig. 3. It was observed that the slip velocity on the wall increases with the Knudsen number. The LBM results are validated against modified Reynolds equation (MRE) in Fig. 3. The MRE was derived from linearized Boltzmann equation [9,10] and the first order MRE solution for the normalized velocity profile for a 2D Couette flow is given as

$$\frac{u}{u_t} = \frac{2y/H - 1}{2Kn + 1} \quad (21)$$

It was observed that the LBM results are in good agreement with the MRE solution for $0.05 < Kn < 5$.

As a second validation case, pressure-driven micro-channel flows have been solved with LBM. Pong et al. [11] fabricated

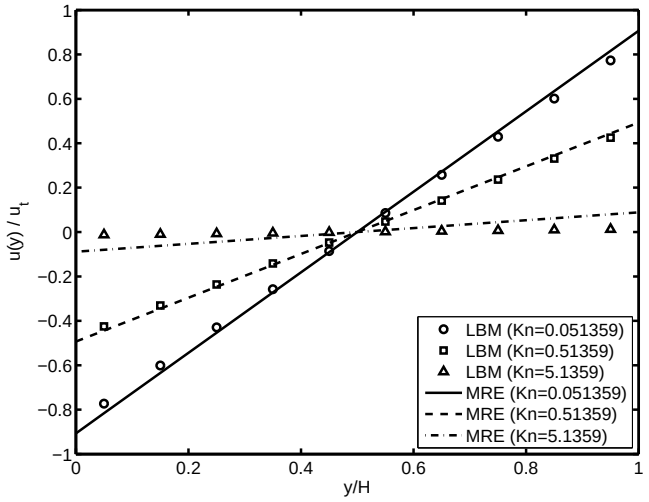

Figure 3. THE NORMALIZED STREAMWISE VELOCITY PROFILE ALONG THE VERTICAL DIRECTION OF THE MICROCHANNEL.

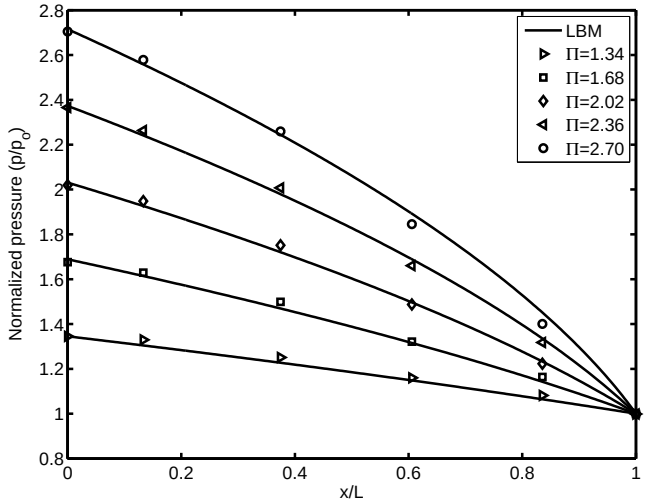

Figure 4. THE NORMALIZED PRESSURE DISTRIBUTION ALONG THE CHANNEL FOR THE EXPERIMENTAL CASE OF PONG ET AL. [11].

a microchannel with integrated pressure and temperature sensors that the measurements of pressure distribution along the microchannels were available. A longer channel system with more number of pressure sensors was used by Shih et al. [12] in order to measure mass flow and axial pressure distribution for helium and nitrogen gases. Also Arkilic et al. [13] have developed a high resolution mass-flow measurement technique for the investigation of gas flow in long microchannels. Our LBM simulation test cases have been based on the experimental conditions given in Table 1. The working gas was Nitrogen and Argon for the cases with $Kn_o = 0.05$ and Helium for $Kn_o = 0.135$. The simulations were in the slip flow regime. The grid size in LBM model was modified according to the experimental dimensions. At the inlet and exit, the densities are set to match the same pressure ratio (Π) used in the experiments. Fig. 4 and Fig. 5 show the LBM results for pressure distribution along the experimental micro channel normalized with exit pressure at various pressure ratios. The pressure distribution is nonlinear as expected for a compressible channel flow. LBM method predicts the pressure distribution accurately compared to the experimental data. In Fig. 4 and Fig. 5, it was observed that the non-linearity of pressure distribution reduces as the Knudsen number increases. This

Table 1. FLOW CONDITIONS AND COMPUTATIONAL PARAMETERS FOR MICRO-POISEUILLE FLOW

Case:	Pong et al. [11]	Shih et al. [12]	Arkilic et al. [13]
Gas:	N_2	He	Ar
H (μm):	1.2	1.2	1.33
L (μm):	3000	4000	7490
p_o (Pa):	1.01×10^5	1.00×10^5	1.01×10^5
Kn_o :	0.05	0.135	0.05
Grid:	12×250	12×400	12×700

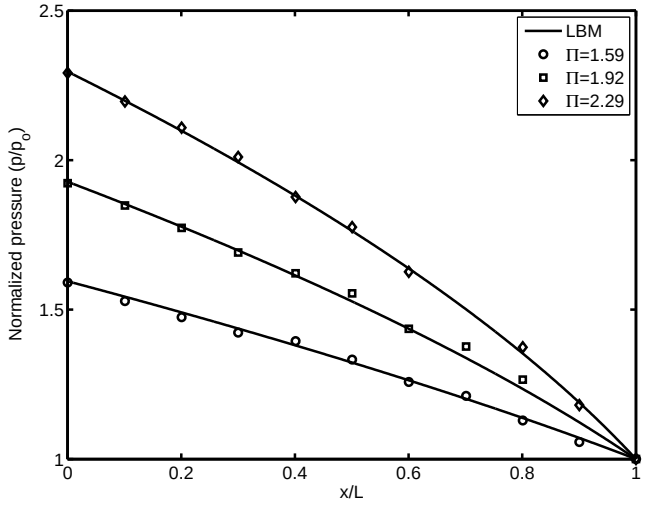

Figure 5. THE NORMALIZED PRESSURE DISTRIBUTION ALONG THE CHANNEL FOR THE EXPERIMENTAL CASE OF SHIH ET AL. [12].

behavior confirms previous findings that the effect of compressibility reduces as the flow becomes more rarefied [14]. In these simulations, the density and the slip velocity at the wall boundary is imposed using following analytical relations for pressure [13] and velocity [14]

$$\tilde{p}(x) = -6\sigma Kn_o + \sqrt{(6\sigma Kn_o)^2 + (1+12\sigma Kn_o)\tilde{x} + (\Pi^2 + 12\sigma Kn_o\Pi)(1-\tilde{x})}, \quad (22)$$

$$\frac{u(y)}{u_c} = \left[-\left(\frac{y}{H}\right)^2 + \frac{y}{H} + \frac{Kn_o}{1+Kn_o} \right] / \left(\frac{1}{4} + \frac{Kn_o}{1+Kn_o} \right). \quad (23)$$

The effective density and velocity at the outer solid nodes were calculated using Eq. 22 and Eq. 23 as

$$\rho_{eff}(x) = \rho_o \tilde{p}(x) \quad (24)$$

$$u_{eff}(x) = 2u(x, N_y/2)\frac{u(H)}{u_c} - u(x, N_y - 1). \quad (25)$$

Next, we calculate the steady-state mass flow rate at the exit section of the channel as $\dot{m}/W = \sum \rho(Nx-1,y)u(Nx-1,y)\Delta y$ and compare them with those predicted by the analytical equation and the experimental data. A solution for the mass flow rate per width ($\dot{m}/W$) for pressure-driven micro-Poiseuille flow was driven by Arkilic *et al.* [15] as

$$\frac{\dot{m}}{W} = \frac{H^3 p_o^2}{24\mu LRT}\left[\Pi^2 - 1 + 12\frac{2-\sigma}{\sigma}Kn_o(\Pi - 1)\right], \quad (26)$$

where W is the width of the channel and σ is taken as unity. Fig. 6 and Fig. 7 display the mass flow rate at various pressure ratios for the micro-Poiseuille flow. The mass flow rate is normalized with the value at the largest pressure ratio. It is found that the present results are in good agreement with the experimental data and analytical predictions. The dashed lines in Fig. 6 and Fig. 7 show the variation of mass flow rate for $Kn_o = 0$. It can be seen that the increase in the mass flow rate due to rarefaction is well captured by the LBM method.

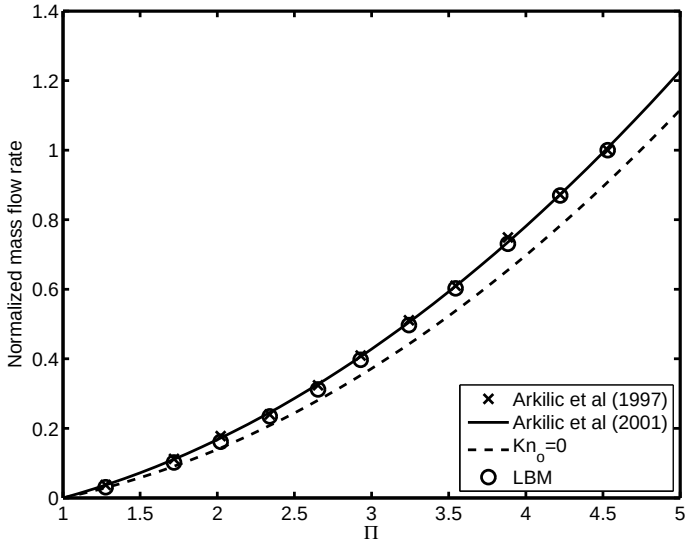

Figure 6. THE NORMALIZED MASS FLOW RATE PER WIDTH AS A FUNCTION OF PRESSURE RATIOS FOR $Kn_o = 0.05$.

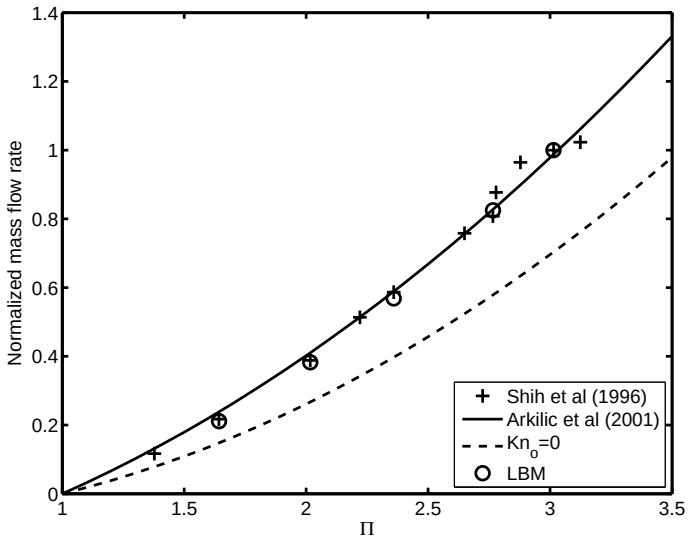

Figure 7. THE NORMALIZED MASS FLOW RATE PER WIDTH AS A FUNCTION OF PRESSURE RATIOS FOR $Kn_o = 0.135$.

Conclusions

In conclusion, isothermal gas flows in two-dimensional microchannels are simulated using a lattice Boltzmann method with effective density and velocity values imposed on the solid nodes. The characteristics of velocity, nonlinear pressure and mass flow rate are examined for micro-Couette and micro-Poiseuille flows. The rarefaction effects on slip velocity and mass flow rate are well captured by the current LBM implementation and the results are validated against experimental and analytical predictions. The type of boundary treatment used in this study enables the implementation of coupled simulations where the flow properties at the regions near the wall can be obtained by other numerical methods such as the Direct Simulation Monte Carlo method. For future study, we will focus on replacing Eq. 22 and Eq. 23 with the results obtained from DSMC simulations. This will enable to increase the range of applicability of the LBM method to other geometries.

REFERENCES

[1] Bird, G. A., 1994. *Molecular Gas Dynamics and the Direct Simulation of Gas Flow*. Clarendon Press, Oxford, U.K.

[2] Gad-el Hak, M., 1999. "Fluid mechanics of microdevices-the freeman scholar lecture". *Journal of Fluids Engineering, Transactions of the ASME,* **121**(1), pp. 5 – 33.

[3] Nie, X., Doolen, G. D., and Chen, S., 2002. "Lattice-boltzmann simulations of fluid flow in mems". *Journal of Statistical Pyhsics*, **107**, pp. 279–289.

[4] Lim, C., Shu, C., Niu, X., and Chew, Y., 2002. "Application of lattice boltzmann method to simulate microchannel flows". *Physics of Fluids*, **14**(7), pp. 2299 – 2308. Microflows;.

[5] Zhang, Y., Qin, R., and Emerson, David, R., 2005. "Lattice boltzmann simulation of rarefied gas flows in microchannels". *Physical Review E - Statistical, Nonlinear, and Soft Matter Physics,* **71**(4), pp. 047702 –.

[6] Bhatnagar, P. L., Gross, E. P., and Krook, M., 1954. "A model for collision processes in gases. i. small amplitude processes in charged and neutral one-component systems". *Pyhsical Review,* **94**(3), pp. 511–525.

[7] Gokaltun, S., Skudarnov, P. V., Sukop, M. C., and Dulikravich, G. S., 2007. "Statistical modeling of rarefied gas channel flows.". In Proceedings of the 18th AIAA Computational Fluid Dynamics Conference.

[8] Zou, Q., and He, X., 1997. "On pressure and velocity boundary conditions for the lattice boltzmann bgk model". *Physics of Fluids,* **9**(6), pp. 1591 –.

[9] Fukui, S., and Kaneko, R., 1987. "Analysis of ultra-thin gas film lubrication based on the linearized boltzmann equation: (influence of accommodation coefficient).". *JSME International Journal,* **30**(268), pp. 1660 – 1666.

[10] Kang, S.-C., Crone, R. M., and Jhon, M. S., 1999. "New molecular gas lubrication theory suitable for head-disk interface modeling". *Journal of Applied Physics,* **85**(8 II B), pp. 5594 – 5596.

[11] Pong, K.-C., Ho, C.-M., Liu, J., and Tai, Y.-C., 1994. "Non-linear pressure distribution in uniform microchannels". *American Society of Mechanical Engineers, Fluids Engineering Division (Publication) FED,* **197**, pp. 51 – 56.

[12] Shih, J. C., Ho, C.-M., Liu, J., and Tai, Y.-C., 1996. "Monatomic and polyatomic gas flow through uniform microchannels". *American Society of Mechanical Engineers, Dynamic Systems and Control Division (Publication) DSC,* **59**, pp. 197 – 203.

[13] Arkilic, E., Schmidt, M., and Breuer, K., 1997. "Gaseous slip flow in long microchannels". *Journal of Microelectromechanical Systems,* **6**(2), pp. 167 – 178.

[14] Karniadakis, G., and Beskok, A., 2001. *Micro Flows: Fundamentals and Simulation*. Springer-Verlag, NY, U.S.A.

[15] Arkilic, E., Breuer, K., and Schmidt, M., 2001. "Mass flow and tangential momentum accomodation in silicon micromachined channels". *Journal of Fluid Mechanics,* **437**(437), pp. 29 – 43.

NOMENCLATURE

c	Lattice speed
$\mathbf{e_a}$	Lattice velocity vector
f_a	Particle density function.
H	Channel height, μm
Kn	Knudsen number.
L	Channel length, μm
$\dot{m}/W$	Mass flow rate per width, $kg/s.m$
Ny	Grid size in the normal direction
Nx	Grid size in the stream direction
p	Pressure, Pa.
$\tilde{p}$	Nondimensional pressure$= p/p_o$
R	Universal gas constant, $J/kg.K$
T	Temperature, K
t	Time, ts
$\mathbf{u}$	Velocity vector
u	Streamwise velocity component
v	Normal velocity component.
W	Channel width, μm
w_a	Weight function in the equilibrium distribution
$\mathbf{x}$	Position vector
$\tilde{x}$	Nondimensional streamwise position$= x/L$

Greek Letters

λ	Mean free path.
Π	Pressure ratio
ρ	Density.
τ	Dimensionless single relaxation time.
τ'	Dimensionless variable relaxation time.
Δt	Time step, ts
σ	Momentum accommodation coefficient

Subscripts and Superscripts

a	Directions on D2Q9 lattice
b	Bottom
c	Center
eq	Equilibrium
eff	Effective
in	Inlet
out	Outlet
o	Channel exit